

Electrophoresis and Electroosmosis in the Intracellular Transport of Macromolecules

Victor P. Andreev*^{1,2,3}

¹ Department of Psychiatry and Behavioral Sciences, University of Miami Miller School of Medicine

² Department of Biochemistry and Molecular Biology, University of Miami Miller School of Medicine

³ Center for Computational Sciences, University of Miami

*Corresponding author: 1120 NW 14th Street, room 1476, Miami, FL 33136, vandreev@med.miami.edu

Abstract: It is a well known fact in capillary electrophoresis and microfluidics that the electroosmotic transport of a typical protein is much faster than the electrophoretic one. However, the role of electroosmosis in the intracellular transport of proteins is neglected. The goal of this paper is to illustrate the importance of electroosmosis in the intracellular transport of macromolecules by creating a simple model and simulation of intracellular transport in the polarized cell.

Keywords: electroosmosis, electrophoresis, proteins, cytoplasm, intracellular transport.

1. Introduction

Electric fields are present in biological systems at multiple spatial and temporal scales. The most widely known is membrane potential resulting from the activity of ion channels. As stated in [1], “in the case of the ion pump/channel activity being asymmetrically distributed, the cell behaves as a miniature electrophoresis chamber”. This statement was confirmed with the recently introduced nanoparticles with encapsulated voltage-sensitive fluorescent dyes, which enabled the measurements of electric field throughout the entire volume of living cell [2]. Recent paper [3] argues that the transport of messenger proteins from the membrane to nucleus is dominated by the electrophoretic motion in the cytoplasmic electric fields as estimated from the measurements of [2].

Electroosmotic flow results from the action of electric field on the electrical double layer, formed at the fluid/solid or fluid/membrane interface and characterized by its zeta-potential, ζ . The flow of the fluid results in the movement of the particles immersed in the fluid. The ratio of electroosmotic and electrophoretic mobilities is equal to $\epsilon\epsilon_0\zeta r_s/q$, where q and r_s are the charge and Stokes radius of the particle. For the

physiological value of zeta-potential (-50 mV) and a single charged protein of average size, electroosmotic mobility is 10 times faster than electrophoretic one. Surprisingly, electroosmosis in the intracellular transport of macromolecules has been ignored so far.

2. Description of the Model

We developed a simple model of a polarized cell presenting it as a square with faceted corners and a nucleus in the center (following the schematic presentation of [1]). Ion pump/channel activity was asymmetrically distributed: electric current was entering from the lower horizontal side of the square and leaving the cell through the opposite side of the square. Electric current density in the cytoplasm and the nucleus were governed by the stationary equation of continuity.

Electroosmotic flow in the cytoplasm was determined by the Navier-Stokes equation in the approximation of the creeping flow, while the electric field within the cytoplasm was determined by the above equation of the electric current continuity. The no slip boundary condition was used at the nucleus membrane, while the electroosmotic velocity boundary condition was used at the cellular membrane. The physiological value of zeta-potential (-50 mV) at the cellular membrane was used in the simulations, while the electrical properties of the cytoplasm and nucleus were taken as $\sigma_1=0.25$ S/m, $\epsilon_1=60$; $\sigma_2=0.5$ S/m, $\epsilon_2=120$, following [4], and cytoplasmic viscosity $\eta = 0.0081$ Pa·s following [5].

The transport of the macromolecules in the cytoplasm was described by the diffusion-convection-migration equations, where the velocity fluid was determined from the solution of the above creeping flow equation, and the electrophoretic migration of the charged

macromolecules was governed by the above electric field distribution.

Following [3], we were interested in the transport of the messenger proteins from the membrane to the nucleus. We modeled this process by introducing a short pulse (0.01 s) of protein concentration at the lower left corner of the cellular membrane and simulating the evolution of the concentration in the presence ($\zeta=-0.05$ V) and in the absence ($\zeta=0$) of the electroosmotic flow.

Further, we were interested in how the “crowded environment” in the cytoplasm could influence the role of electroosmosis in the intracellular transport. With this in mind we developed a simple model mimicking the organization of mammalian cytoplasm described in [6], where the endogenous cytoplasmic proteins formed macromolecular assemblies linked to the actin cytoskeleton. Then we simulated the transport of messenger proteins in this environment, allowing the competition of the proteins for the cytoskeleton binding sites.

3. Use of COMSOL Multiphysics

COMSOL is well suited for the simulation of electroosmosis. Several COMSOL models of electroosmotic flow in microfluidic devices have been published, including [7]. In our simulation, we took advantage of the presence of electroosmotic velocity boundary condition in the Microfluidics module of COMSOL 4.2. Our model includes the following physics interfaces: Electric Currents, Creeping Flow, and Transport of Diluted Species; the first two in the stationary and the last one in the time dependent mode.

4. Results

Figure 1 represents electric potential and electroosmotic flow velocity in our simple model of the polarized cell. The maximum of electroosmotic flow is, as expected, along the cellular membrane – in the model the vertical sides of the square (from the bottom to the top), while the reverse flow is mostly along the center line of the square. The presence of the nucleus (with the no slip boundary condition at the nucleus membrane) slightly disturbed the flow relative to the well known profile, (e.g. in a

cylinder with the closed ends). We experimented with the positioning of the nucleus (data not shown) and got predictable disturbances of the electroosmotic flow along the center line of the square without much effect on the flow along the membrane.

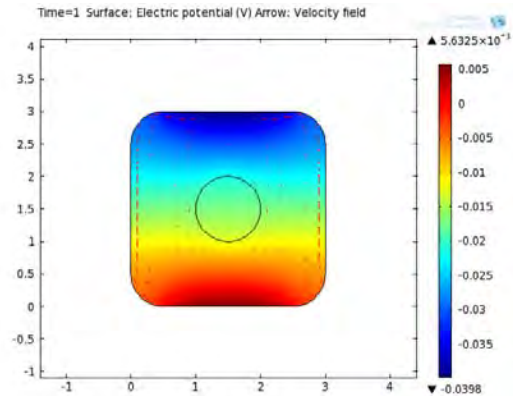


Figure 1. Electrical potential and flow velocity in a simple model of polarized cell. Size: $3\mu\text{m}$, membrane zeta-potential: -50 mV. The potential difference of 45 mV from the top to the bottom of the cell is due to asymmetric activity of the ion channels.

Figures 2 and 3 represent the distribution of the messenger protein concentration and the total protein flux at times $t=0.1\text{s}$ and $t=1\text{s}$ initiated by a short impulse (0.01s) of protein concentration at the “corner” of cellular membrane. Electric field distribution and electroosmotic flow velocity are taken from the solution presented in Figure 1.

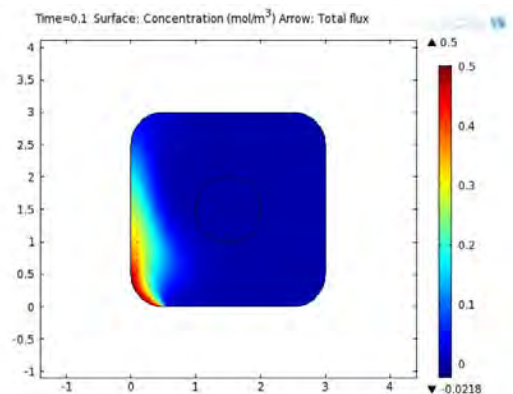


Figure 2. Concentration and flux of messenger protein at time $t=0.1\text{s}$. Diffusion coefficient: $10^{-12}\text{m}^2/\text{s}$, charge: single negative, $\zeta=-0.05$ V.

Figure 4 represents the distribution of the same messenger protein when electroosmotic flow is neglected. The easiest way to model it is to assume zeta-potential equals zero.

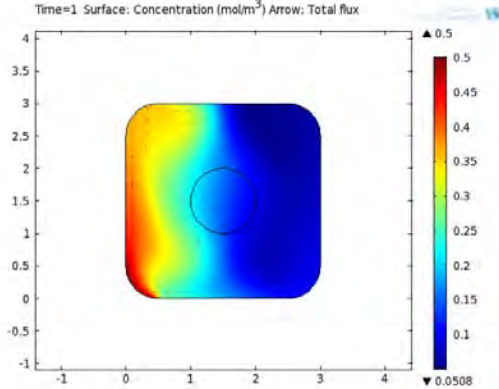


Figure 3. Concentration and flux of messenger protein at time $t=1s$. Diffusion coefficient: $10^{-12}m^2/s$, charge: single negative. $\zeta=-0.05 V$.

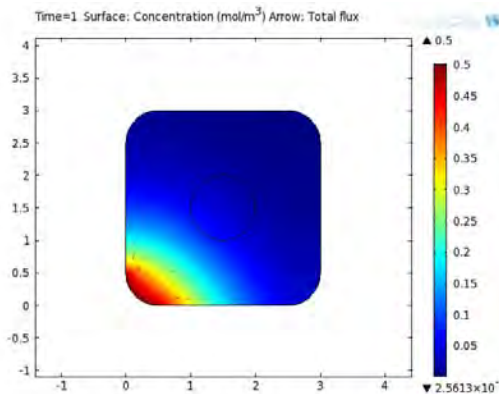


Figure 4. Concentration and flux of messenger protein at time $t=1s$. For comparison with Figure 3, electroosmosis is ignored here ($\zeta=0$, transport is by diffusion and electrophoresis).

Protein molecules in the presence of electroosmosis are distributed over a much larger part of the cytosol than when the transport is only due to diffusion and electrophoresis. The amount of protein molecules that reached nucleus by $t=1s$ is 3-fold higher in the presence of electroosmosis.

The recent paper [6] presented the experiment that investigated the release of the proteins after gentle permeabilization of the cellular membranes of Chinese hamster ovary cells with saponin, which allowed entry of molecules of at least 800 kDa. The measurements of the rate of release of

endogenous proteins showed that protein release was slow: around 10% of total protein amount left cytoplasm after 10 minutes and about 25% after an hour after permeabilization of the membrane. This observation supported the conclusion that endogenous proteins in mammalian cytoplasm are normally not free to diffuse over large distances due to bonding to cytoskeleton [6].

To study how bonding to cytoskeleton influences the intracellular transport of proteins we developed a simple model mimicking the experiment of [6]. First of all, importantly, the process of permeabilization of the cellular membrane makes it permeable to small ions, and therefore eliminates any charged double layer and membrane potential. Therefore, electroosmosis is eliminated in the saponin treated cells. Similarly, permeability to small ions eliminates polarization of the cells and therefore electric field and electrophoresis are also absent. All transport is by diffusion then. Permeable cellular membrane was mimicked by setting the endogenous protein concentration $C_e=0$ at the cellular membrane.

We represented binding of endogenous protein to the immobilized cytoskeleton binding sites by the following second order reaction term introduced into the diffusion-reaction equations. C_2 - concentration of the free sites, C_3 - concentration of the sites occupied by endogenous proteins.

$$R_e = -k_1 C_e C_2 + k_{r1} C_3 = R_2 = -R_3$$

Figure 5 represents the rate of release of endogenous protein from the cytoplasm

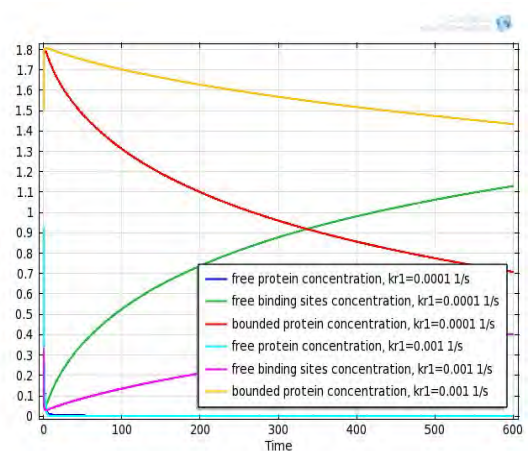


Figure 5. Concentrations of endogenous protein C_e , free binding sites C_2 , and occupied binding sites C_3 versus time in seconds. Initial values: $C_e=1\text{mM}$, $C_2=1\text{mM}$, $C_3=1\text{mM}$, $k_1=1\text{ m}^3/(\text{mol}\cdot\text{s})$

As seen, the equilibrium ratio between the free and bonded endogenous protein is established during the first couple of seconds and then slow release of the endogenous protein follows with the rate determined by the reverse reaction rate k_{r1} . The value of $k_{r1}=0.001\text{s}^{-1}$ predicts release rate consistent with the observations of [6].

Having evaluated the plausible reverse reaction rate for endogenous proteins, we then modeled the transport of messenger protein in the “crowded environment”. As previously, we introduced messenger protein at the lower left “corner” of the cellular membrane. Now in addition to transport by electroosmosis, electrophoresis and diffusion, messenger molecules spend part time bonded to the cytoskeleton binding sites. We assumed the possible competition between the messenger protein and endogenous protein for the binding sites described by the following reaction term:

$$R_2 = -k_m C_m C_2 + k_{rm} C_5 - k_e C_e C_2 + k_{re} C_3$$

where C_e , C_m , C_2 , C_3 , C_5 – concentrations of free endogenous protein, free messenger protein, free binding sites, binding sites occupied with endogenous proteins, and binding sites occupied by messenger proteins; k_m and k_{rm} – direct and reverse reaction rates for messenger protein, while k_e and k_{re} – direct and reverse reaction rates for endogenous protein.

First we analyzed the situation where the binding sites are in abundance, so the competition between messenger protein and endogenous protein are minimal. Initially, almost all endogenous protein is bonded, while the messenger protein is absent: $C_e=0.001$, $C_m=0$, $C_2=1$, $C_3=1$, $C_5=0$. Messenger protein is introduced at the “corner” of the cellular membrane as a short rectangular pulse: $0.001 \cdot \text{rect}1(0.01)$. All concentrations are in mM. Following the above model representing the observations of [6], we assumed: $k_e=1\text{ m}^3/(\text{mol}\cdot\text{s})$ and $k_{re}=0.001\text{ s}^{-1}$. Also, following the reasoning of [6] we assumed the less strong bonding ($k_{rm}=0.01\text{ s}^{-1}$) for the messenger protein than for endogenous protein.

Figure 6 represents the concentration and the total flux of the messenger protein at time $t=1\text{ s}$. Electroosmosis, electrophoresis, diffusion, and binding to the immobilized binding sites is present. For comparison, Figure 7 presents the messenger concentration and flux in case electroosmosis is absent ($\zeta=0$). Similar to the case without bonding, messenger protein occupies much larger part of the cell in case where electroosmosis is present then in the case where it is absent.

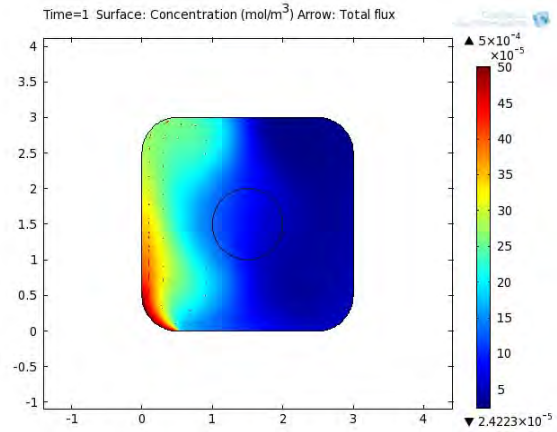


Figure 6. Concentration and flux of messenger protein at time $t=1\text{s}$. Binding sites are in abundance. Equal binding reaction rates for endogenous and messenger proteins: $k_m=k_e=1\text{ m}^3/(\text{mol}\cdot\text{s})$. Diffusion coefficient: $10^{-12}\text{ m}^2/\text{s}$, charge: single negative. Electroosmosis present: $\zeta=-0.05\text{ V}$

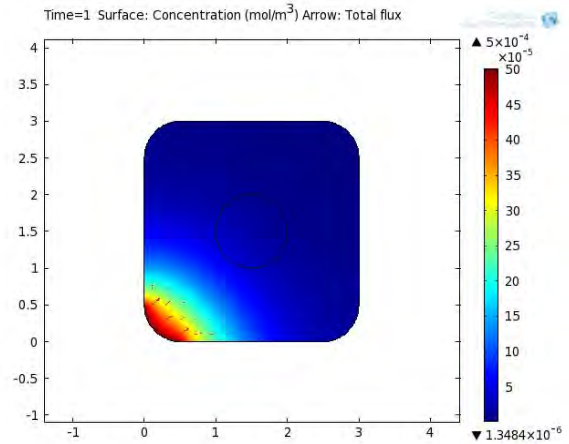


Figure 7. Concentration and flux of messenger protein at time $t=1\text{s}$. Electroosmosis absent: $\zeta=0$. Other conditions the same as in Figure 6.

Comparison of concentration distributions with and without binding reveals similar patterns determined by the electroosmotic flow profile in Figures 3 and 6 ($t=1$, without and with binding). Further, comparison of Figure 6 with Figure 2 ($t=0.1$, without binding, electroosmosis present) demonstrates the similarity of binding case with the case without binding, but at earlier time point, which is reasonable because in case of binding present, the messenger protein molecules spend only part time in the free state where they are able to move with the electroosmotic flow and to diffuse.

Figure 8 presents the amount of messenger protein that reaches the nucleus versus time evaluated in 5 cases: four where electroosmosis is present (of them one without binding of messenger protein and three with various binding reaction rates) and one with electroosmosis neglected and binding present. Comparison of the curves with the same binding reaction rate shows that the amount of messenger protein that reaches nucleus is 6-fold higher in case electroosmosis is present relative to the case where it is absent.

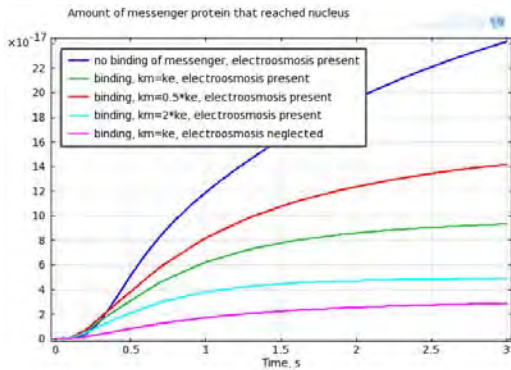


Figure 8. Amount of messenger protein that reached nucleus versus time. Binding sites are in abundance. $C_e=0.001\text{mM}$, $C_2=1\text{mM}$, $C_3=1\text{mM}$, $C_5=0$, $C_m=0.001\text{-rect1}(0.01)\text{ mM}$. $\zeta=-0.05\text{ V}$. $D_e=D_m=10^{-12}\text{m}^2/\text{s}$, $z_e=z_m=-1$. $k_e=1\text{ m}^3/(\text{mol}\cdot\text{s})$ and $k_{re}=0.001\text{ s}^{-1}$, $k_{rm}=0.01\text{ s}^{-1}$.

Then we studied the situation without an abundance of the cytoskeleton binding sites, where the competition between endogenous and messenger proteins could be more important. In this case: initially, free and bonded endogenous proteins are in equilibrium, meaning that practically all the binding sites are occupied:

$C_e=0.045$, $C_2=0.044$, $C_3=1.956$. Messenger protein $C_m=0.01\text{-rect1}(0.01)$. Reaction rates: $k_e=1\text{ m}^3/(\text{mol}\cdot\text{s})$, $k_{re}=0.001\text{ s}^{-1}$, $k_{rm}=0.01\text{ s}^{-1}$; $k_m=k_e$, $k_m=0.5\cdot k_e$, $k_m=2\cdot k_e$. Results are presented in Figure 9.

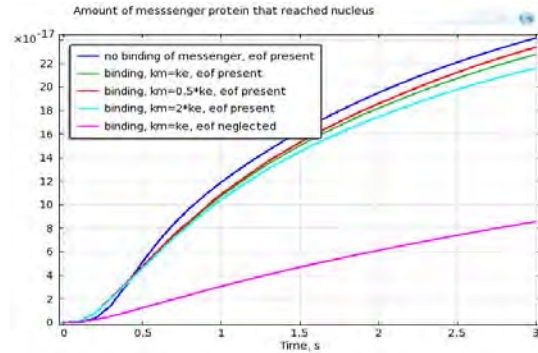


Figure 9. Amount of messenger protein that reached nucleus versus time. Competition for binding sites. Slow binding. $C_e=0.045\text{ mM}$, $C_2=0.044\text{ mM}$, $C_3=1.956\text{ mM}$. $\zeta=-0.05\text{ V}$. $D_e=D_m=10^{-12}\text{m}^2/\text{s}$, $z_e=z_m=-1$. $k_e=1\text{ m}^3/(\text{mol}\cdot\text{s})$ and $k_{re}=0.001\text{ s}^{-1}$, $k_{rm}=0.01\text{ s}^{-1}$.

Here competition between messenger and endogenous proteins for cytoskeleton binding sites is present, binding is rather slow and only small portion of messenger protein molecules have enough time to bind the cytoskeleton sites. Therefore, curves with binding and without binding (electroosmosis present) are rather close (less than 20% difference at $t=1\text{ s}$). Transport without electroosmosis is much slower than with electroosmosis (4-fold at $t=1\text{ s}$).

Figure 10 demonstrates what happens when the binding reaction rate is 10-fold higher.

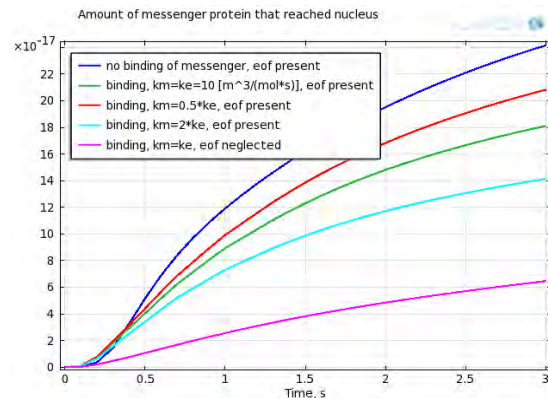


Figure 10. Amount of messenger protein that reached nucleus versus time. Competition for binding sites. Fast binding. $C_e=0.045\text{ mM}$, $C_2=0.044\text{ mM}$, $C_3=1.956$

mM. $\zeta = -0.05$ V. $D_e = D_m = 10^{-12} \text{m}^2/\text{s}$, $z_e = z_m = -1$. $k_e = 1 \text{m}^3/(\text{mol}\cdot\text{s})$ and $k_{re} = 0.001 \text{s}^{-1}$, $k_{rm} = 0.01 \text{s}^{-1}$.

Here binding reaction is 10-fold faster, so more messenger protein molecules are getting bonded and less reach nucleus (25-40% decrease at $t=1$ s relative to Fig 9). Transport without electroosmosis is much slower than with electroosmosis (4-fold less protein reaches nucleus at $t=1$ s).

5. Conclusions

Our simple model shows that electroosmosis can play an important role in the transport of proteins in the cytoplasm of the polarized cells. In our simulation, electroosmosis substantially increases the rate of transport (relative to diffusion and electrophoresis) of messenger proteins from the cellular membrane to the nucleus, both in the case of free messenger proteins (3-fold) and in the case of the messenger protein binding cytoskeleton sites with or without competition for the sites with the endogenous proteins (4-6-fold).

Further modeling studies of intracellular transport in more realistic cellular shapes and in the presence of cellular organelles are obviously necessary and will follow. Further, we plan to measure the cytoplasmic electric field distributions by using the technology of [2] and incorporate it into the more detailed model. Although the electric field distribution and the electroosmotic flow pattern might change due to the more detailed studies and certainly could differ across the cell types, we believe that it would not change the conclusion that electroosmosis is an important factor in the intracellular transport and should not be ignored.

8. References

1. A. De Loof. The cell as a miniature electrophoresis chamber. *Comp. Biochem. Physiol.*, **80A**, 453-459 (1985).
2. K.M. Tyner, R. Kopelman *et al.* Nanosized voltmeter enables cellular-wide electric field mapping. *Biophys J*, **93**, 1163-1174 (2007).
3. R.A. Gatenby, B.R. Frieden. Coulomb interactions between cytoplasmic electric fields and phosphorylated messenger proteins optimize information flow in cells. *Plos One*, **5**, e12084 (2010).

4. A.L. Garner, G. Chen, N. Chen, V. Sridhara, J.F. Kolb, R.J. Swanson, S.J. Beebe, R.P. Joshi, K.H. Schoenbach. Ultrashort electric pulse induced changes in cellular dielectric properties. *Biochem Bioph Res Co*, **362**, 139-144 (2007).
5. I. Lang, M.Scholz, R.Peters. Molecular mobility and nucleoplasmic flux in hepatoma cells. *J Cell Biol*, **102**, 1183-1190 (1986).
6. A. Hudder, L. Nathanson, M.P. Deutscher. Organization of mammalian cytoplasm. *Mol Cell Biol*, **23**, 9318-9326 (2003).
7. H. Chen, Y.T. Zhang, I. Mezic, C.D. Meinhardt, and L. Petzold, Numerical Simulation of an Electroosmotic Micromixer. *Proc Microfluidics 2003 (ASME IMECE)*, (2003).